Advanced modelling of short-fibre reinforced composites

ZUZANA MURČINKOVÁ[1*], VLADIMÍR KOMPIŠ[2]

In this paper, a Method of External Finite Element Approximation (MEFEA) to model such problems like composites reinforced by short fibres will be presented. MEFEA is an enhanced classic FEM with idea of external approximations. There are shape functions in the discrete solution space that do not belong to the infinite dimensional solution space. The domain is split in subdomains (cells) and the approximation is built on each of these subdomains independently of each other. The method is similar to Hybrid Trefftz Finite Element Method, where Trefftz functions are used inside each element (subdomain). The displacement and force boundary conditions are met only approximately whereas the governing equations are fulfilled exactly in the volume for linear elasticity, making it possible to assess accuracy in terms of error in boundary conditions. The main benefit is that the discretization can be done directly on a 3D CAD geometry with all details (features) for the analysis.

Key words: subdomain, Trefftz functions, fibre reinforced composite, reinforcing effect

1. Introduction

Boundary-type solution methodologies are now well established as alternatives to prevailing domain-type methods like the FEM [3, 14] because of computational advantages they offer by the reduction of the dimensionality and good accuracy for the whole domain and simplifying data preparation for the model.

We deal with special type of domain, specifically the composite material, typical for its non-homogeneous structure. In the next part, the state of art of Trefftz-type methods is described. The MEFEA is Trefftz-type method applied to fibre reinforced composites.

The Hybrid-Trefftz methods [5, 7, 9, 12] are boundary-type methods. They use a set of trial functions, singular or non-singular, which a priori satisfy corresponding

[1] Department of Technical Devices Design, Faculty of Manufacturing Technologies of Technical University Košice with seat in Prešov, Slovak Republic

[2] Department of Mechanical Engineering, Academy of the Armed Forces, Liptovský Mikuláš, Slovak Republic

[*] Corresponding author, e-mail address: murcinkova@kryha.sk

linear part of the governing differential equation inside the (sub-) domain (large element).

The Method of Fundamental Solutions (MFS) [6, 8] is a boundary meshless method that does not need any mesh in classical FEM meaning and in linear problems, only nodes (collocation points) on the domain boundaries and a set of source functions (fundamental solutions) in points outside the domain are necessary to satisfy the boundary conditions. MFS has certain advantages over the BEM, as it completely avoids the need for any integral evaluation and it leads to very simple formulations in some problems. However, large number of both collocation points and source functions are necessary, if the shape of the domain is complicated and moreover, the resulting system of equations is ill-conditioned in some problems. The source functions serve as the trial functions and are to be placed outside the domain. The location of the source functions is vital to both the accuracy and numerical stability of the solution. The MFS can be also included to Trefftz-type methods.

Another boundary-type meshless method – the Boundary Point Method (BPM) was developed in [10]. The BPM is based on the direct formulation of conventional and hypersingular BIE employing favourable features of both the MFS and BEM. It is well known that for the integration of kernel functions over boundary elements, the shorter the distance between the source and field points, the more difficult it is to evaluate them accurately because of the properties of fundamental solutions. In the formulation "moving elements" are introduced by organizing relevant adjacent nodes in order to describe the local features of a boundary such as position, curvature and direction, over which the treatment of singularity and integration can be carried out, a benefit not only for evaluating of integrals in the case of coincidence points, but also for the versatility afforded by using unequally spaced nodes along the boundary.

In this paper, an important application of the MEFEA (involved in Procision software) to model such problems like fibre reinforced composites will be presented and it will be compared to the solution of the problem with displacement-based isoparametric FEM with polynomial order refinement (p-FEM [14]).

The MEFEA and description of subdomains are comprised in Chapter 2, numerical results, computation of reinforcing effect, description of mechanical behaviour and comparison of MEFEA with p-FEM results are presented in Chapter 3 and conclusions are given in Chapter 4.

2. The method of external finite element approximation

The MEFEA uses specific finite elements called subdomains (cells) of arbitrary shape. Ce'a introduced the idea of external approximation in 1964 [4]. The method was developed by Aubin (1972) [2] and Apanovitch (since 1981) [1].

The MEFEA is an enhanced classic FEM with idea of external approximations. The method does not need discretization by classical elements, however instead of elements the domain is divided into subdomains. The main benefit is that the discretization can be done directly on a 3D CAD geometry without any defeaturing, clean up or simplifications of geometry. The geometry can be left intact with all the details in it for the analysis.

The method is familiar to Hybrid Trefftz Finite Element Method (HT-FEM) [5, 7, 9], where Trefftz functions are used inside elements. The displacement and force boundary conditions are met only approximately whereas the governing equations are fulfilled exactly in the volume for linear elasticity, making it possible to assess accuracy in terms of error in boundary conditions.

2.1 Description of subdomain

The subdomains can be recognized as large Trefftz elements since the Trefftz functions are used inside each finite element – subdomain. In this paper, the subdomains are named also as Apanovitch elements. It is also similar to hybrid-Trefftz elements as defined by Jirousek [7] with a little different derivation of the elements. Apanovitch definition of the formulation is kept in this paper.

The domain is split into several subdomains and the approximation is built on each of these subdomains independently of each other. It means that each subdomain has its own set of approximation functions. Then, at the interface of the subdomains, the discrete solution may be discontinuous (and therefore does not belong to the solution space). But then these discontinuities can be penalized by using, for example, Lagrange multipliers and get a solution that is 'almost continuous' across the interface between two subdomains (i.e. the continuity is then satisfied in the weak, integral sense).

The disadvantage is that in case of not properly divided domain, the matching of the approximations at the interfaces is less accurate and it needs another improvement of 'mesh'.

The examples of subdomains used in the MEFEA are presented in Fig. 1.

According to weak formulation of the boundary value problem, it is necessary to find function $u \in V$, which fulfils the abstract variation equation:

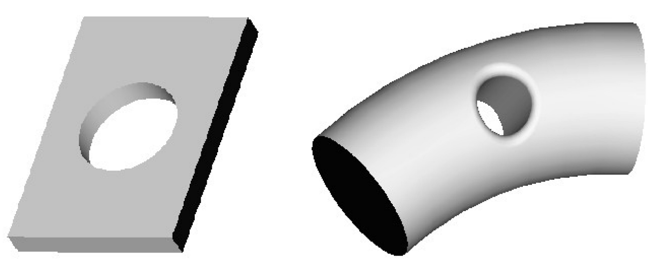

Fig. 1. Subdomains.

$$a(u, v) = f(v) \quad \text{for any function} \quad v \in V, \tag{1}$$

where V is the infinite dimensional solution space, $a(u, v)$ is generally an unsymmetrical bilinear form which is continuous on the space product $V \times V$ and $f(v)$ is some linear form on V.

We can find function $u \in V$ using the numerical methods and discretization of weak formulation. We replace function u by its approximate U_{h}:

$$U_{\mathrm{h}} = \sum_{i=1}^{n} C_i^{(\mathrm{h})} N_i^{(\mathrm{h})} \quad \text{from space} \quad X_{\mathrm{h}}, \tag{2}$$

where $C_i^{(\mathrm{h})}$ and $N_i^{(\mathrm{h})}$ are factors and basis functions, respectively.

Factors $C_i^{(\mathrm{h})}$ in Eq. (2) are called degrees of freedom. In conventional Finite Element Method, factors $C_i^{(\mathrm{h})}$ are displacements of the nodes (or temperature). It means $C_i^{(\mathrm{h})}$ have physical meaning. In classical Ritz-Galerkin method, the factors $C_i^{(\mathrm{h})}$ have no physical meaning and no relation to any geometric entity.

In MEFEA the degrees of freedom have no physical meaning and further continuity of the field variable is not necessary. The method only insists that approximate continuity and approximate fulfilment of the essential boundary conditions be achieved. The unknowns C_i are not limited to being simple parameters. They may alternatively be unknown of one of the independent variables.

There are three types of the degrees of freedom in the MEFEA: Boundary Degrees of Freedom, Internal Degrees of Freedom and Concentrator Degrees of Freedom.

2.1.1 Boundary Degrees of Freedom

Boundary degrees of freedom are factors responsible for the satisfaction of the displacement conditions and continuity conditions on the dividers of subdomains (along their common surfaces). The more degrees of freedom which are used to model the boundary conditions, the closer they are approximated. They are defined by integral:

$$C_i = \int_S G_i U \,\mathrm{d}S, \tag{3}$$

where S is either the boundary of the domain or a divider surface, G_i are some basis functions defined on the surface and U is the function to be approximated (displacement, temperature).

The number of boundary degrees of freedom is increased, if the quality of boundary condition fulfilment does not meet the convergence criteria.

2.1.2 Internal Degrees of Freedom

Internal degrees of freedom are factors responsible for satisfaction of force boundary conditions and for quality of the global solution. These factors have no physical meaning and they are associated with volume of a subdomain.

2.1.3 Concentrator Degrees of Freedom

Concentrator degrees of freedom are factors responsible for the accurate simulation of the stress state near a stress concentrator. These factors have no physical meaning and they correspond to special basis functions as:

$$U_\mathrm{h} = \sum_{i=1}^{n} C_i^{(\mathrm{h})} N_i^{(\mathrm{h})} + \sum_{i=1}^{m} c_i f_i, \tag{4}$$

where $f_i = \frac{1}{r}$ is a concentrator basis function and c_i, $1 \leq i \leq m$, are the concentrator degrees of freedom.

Each of the degrees of freedom described above is associated with some basis function. These basis functions approximate the solution of boundary value problem. Basis functions in the MEFEA exactly fulfil the governing differential equations of the theory of elasticity in structural analysis or equations of heat conduction in thermal analysis. There are two types of functions: polynomial type and non-polynomial type of special asymptotic behaviour (radial functions) and they are intended to approximate the solution in stress concentration regions.

Whereas in exact solution it is insisted that the field variables itself have to be equal on both sides of the boundary, in the MEFEA it is insisted only that integrals (3) have to be equal.

2.2 Discretization

The examples of subdomains are in Fig. 1. The arbitrary shaped subdomains with piecewise smooth parts of dividers are the "finite elements" – subdomains – Apanovitch elements. The form and increasing number of smooth parts of their dividers increase the solution time; therefore this choice is made only with reason to increase the accuracy of approximation of solved domain boundary. It is necessary to mention that the degrees of freedom are not associated with nodes in the MEFEA, but nodes are needed for definition of subdomain geometry.

2.3 Basis functions of the subdomains

We show the different way of building the basis functions (compared to classical FEM). We describe it according to [1]. To build the basis functions, it is necessary to enter base of initial space P^K and build the space P_Σ (subspace of space P^K) and P_Z (supplement to subspace P_Σ):

$$P^{\mathrm{K}} = P_{\Sigma} + P_{\mathrm{Z}}. \tag{5}$$

Let $P \subset H^m(K)$, where $H^m(K)$ is Sobolev space – space of functions with finite strain energy, P is finite dimensional space, further called as initial function, and $\{N_k\}$, $1 < k < n$ is its base:

$$N = \sum_{k=1}^{n} b_k N_k, \qquad \forall N \in P, \tag{6}$$

where b_k are coefficients.

The matrix $\mathbf{R}$ of the system equations relates the coefficients of initial set of functions and subdomain boundary degrees of freedom by:

$$\mathbf{R}\boldsymbol{b}^{\mathrm{T}} = \boldsymbol{\varphi}^{\mathrm{T}}, \tag{7}$$

where $\mathbf{R}$ is the matrix $m \times n$, $\boldsymbol{b} = (b_k)_{k=1}^{n}$ is vector of coefficients and $\boldsymbol{\varphi} = (\varphi_i)_{i=1}^{m}$ is vector of subdomain boundary degrees of freedom.

The system of Eqs. (7) can be written in the form:

$$\mathbf{R}_{\Sigma}\boldsymbol{b}_{\Sigma}^{\mathrm{T}} + \mathbf{R}_{\mathrm{Z}}\boldsymbol{b}_{\mathrm{Z}}^{\mathrm{T}} = \boldsymbol{\varphi}^{\mathrm{T}}, \tag{8}$$

where $\mathbf{R}_{\Sigma}$ is matrix $m \times m$ and $\mathbf{R}_{\mathrm{Z}}$ is matrix $m \times (n-m)$.

Multiplying Eq. (8) by matrix $\mathbf{R}_{\Sigma}^{-1}$ from the left, we obtain the vector $\boldsymbol{b}_{\Sigma}$ by means of vectors $\boldsymbol{b}_{\mathrm{Z}}$ and $\boldsymbol{\varphi}$ as

$$\boldsymbol{b}_{\Sigma}^{\mathrm{T}} = \mathbf{R}_{\Sigma}^{-1}\boldsymbol{\varphi}^{\mathrm{T}} - \mathbf{R}_{\Sigma}^{-1}\mathbf{R}_{\mathrm{Z}}\boldsymbol{b}_{\mathrm{Z}}^{\mathrm{T}}. \tag{9}$$

The expression (8) can be written:

$$\mathbf{N} = \mathbf{N}_{\Sigma}\boldsymbol{b}_{\Sigma}^{\mathrm{T}} + \mathbf{N}_{\mathrm{Z}}\boldsymbol{b}_{\mathrm{Z}}^{\mathrm{T}}, \tag{10}$$

where $\mathbf{N}_{\Sigma} = (N_k)_{k=1}^{m}$ and $\mathbf{N}_{\mathrm{Z}} = (N_k)_{k=n-m+1}^{n}$.

Substituting (9) into (10), we get:

$$\begin{aligned} \mathbf{N} &= \mathbf{N}_{\Sigma}\mathbf{R}_{\Sigma}^{-1}\boldsymbol{\varphi}^{\mathrm{T}} + \left(\mathbf{N}_{\mathrm{Z}} - \mathbf{N}_{\Sigma}\mathbf{R}_{\Sigma}^{-1}\mathbf{R}_{\mathrm{Z}}\right)\boldsymbol{b}_{\mathrm{Z}}^{\mathrm{T}} \\ &= \sum_{k=1}^{m} \varphi_k(\mathbf{N}) \left(\sum_{i=1}^{m} N_i r_{ik\Sigma}\right) + \sum_{j=1}^{n-m} b_j^{\mathrm{Z}} \left(N_{j+m} - \sum_{l=1}^{m} N_l \sum_{k=1}^{m} r_{lk\Sigma} r_{kj\mathrm{Z}}\right), \end{aligned} \tag{11}$$

where $r_{ik\Sigma}$, $(1 < i, k < m)$ are elements of matrix $\mathbf{R}_\Sigma^{-1}$ and $r_{kj\mathrm{Z}}$, $(1 < k < m$, $1 < j < n - m)$ are elements of matrix $\mathbf{R}_\mathrm{Z}$.

In this way we obtain decomposition of $\mathbf{N} \in P = P^\mathrm{K}$ into elements of the new base. We get basis functions of space P_Σ:

$$\mathbf{N}_{k\Sigma} = \sum_{i=1}^{m} N_i r_{ik\Sigma}, \qquad 1 < k < m, \tag{12}$$

where $N_{k\Sigma}$ are basis functions of space P_Σ, $r_{ik\Sigma}$ are elements of matrix $\mathbf{R}_\Sigma^{-1}$ and basis functions of space P_Z are:

$$N_{j\mathrm{Z}} = N_{j+m} - \sum_{l=1}^{m} N_l \sum_{k=1}^{m} r_{lk\Sigma} r_{kj\mathrm{Z}}, \qquad 1 < j < n - m, \tag{13}$$

where $N_{j\mathrm{Z}}$ are basis functions of space P_Z, and $r_{kj\mathrm{Z}}$ $(1 < k < m$, $1 < j < n - m)$ are elements of $\mathbf{R}_\mathrm{Z}$.

We can see that for building the bases $\{N_{k\Sigma}\}_{k=1}^{m}$ and $\{N_{j\mathrm{Z}}\}_{j=1}^{n-m}$ it is necessary to enter base $\{N_i\}_{i=1}^{n}$ of initial space P^K.

3. Numerical results

We focus on simulation of mechanical behaviour of composite materials reinforced by regularly distributed straight unidirectional overlapping fibres using the MEFEA.

3.1 Description of computational models

Using the symmetry, a part of model in Fig. 2 is taken for numerical simulation. The model is 3D solid model. The fibres are straight, cylindrical and regularly distributed with overlapped configuration as indicated in Fig. 2. The ends of each fibre are modelled as half-sphere to avoid singularity. The ideal cohesion between matrix and fibre is assumed. The authors often introduce such form to simulate materials reinforced by carbon nano-tubes (CNT) [11, 13].

The material of both matrix and fibre is considered to be isotropic linear elastic. The interface between fibre and matrix is considered as perfect therefore the fibre and matrix create the continous material without gaps and slip between the matrix and fibre.

We decided to use the dimensionless model by reason that the model was linear and in this manner we could re-calculate results for arbitrary material. Such approach is common in scientific literature.

The constant displacement in the direction of fibre axis (y) equal to $5 \cdot 10^5$ is prescribed in the whole upper surface. The matrix and fibre modulus of elasticity ratio are $1 : 10^2$, $1 : 10^3$ and $1 : 10^4$, Poisson's ratio $\mu = 0.27$. The length of fibres is $L = 50$ and the radius $R = 1$, i.e. the aspect ratio $(2 * R : L)$ is $1 : 25$. The distance

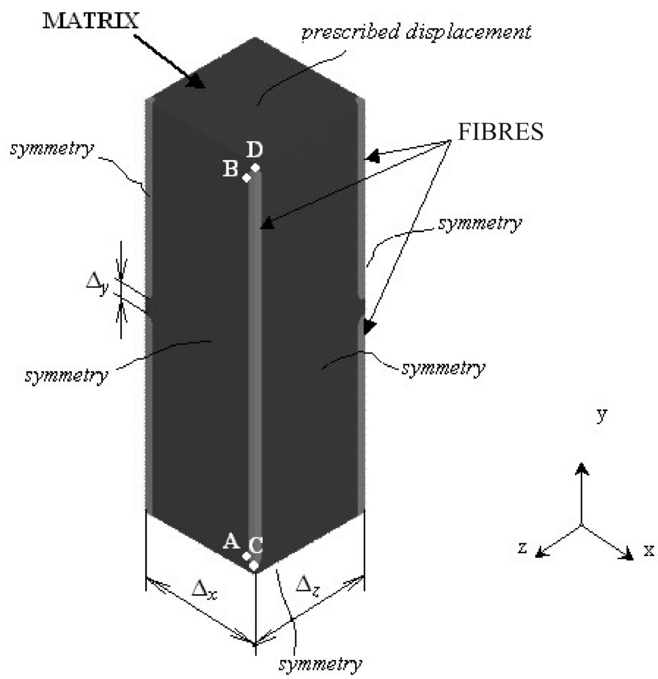

Fig. 2. 3D model.

between fibres is $\Delta_x = \Delta_z = 10$ in the first model and is $\Delta_x = \Delta_z = 16$ in the second model, $\Delta_y = 2$ is for both models (Table 1). The fibres in the representative volume contain only 1.2 vol.% ($16R$) of the volume of the composite material in the first model and 3 vol.% ($10R$) in the second model (Table 1).

Displacements and stresses are evaluated along lines AB and CD in order to obtain information on reinforcing effect as well as on accuracy of used numerical models. Because of the regularly distributed fibres and symmetry conditions, the

T a b l e 1. Model parameters

Model	% fibre of the volume	Distance between fibres	Length of fibres	Radius	$E^{\mathrm{m}} : E^{\mathrm{f}}$	Poisson's ratio
1.	1.2 vol.%	$\Delta_x = \Delta_z = \mathbf{16}$ $\Delta_y = \mathbf{2}$	50	1	$1 : 10^2$	$\mu = 0.27$
2.	3.0 vol.%	$\Delta_x = \Delta_z = \mathbf{10}$ $\Delta_y = \mathbf{2}$			$1 : 10^3$ $1 : 10^4$	

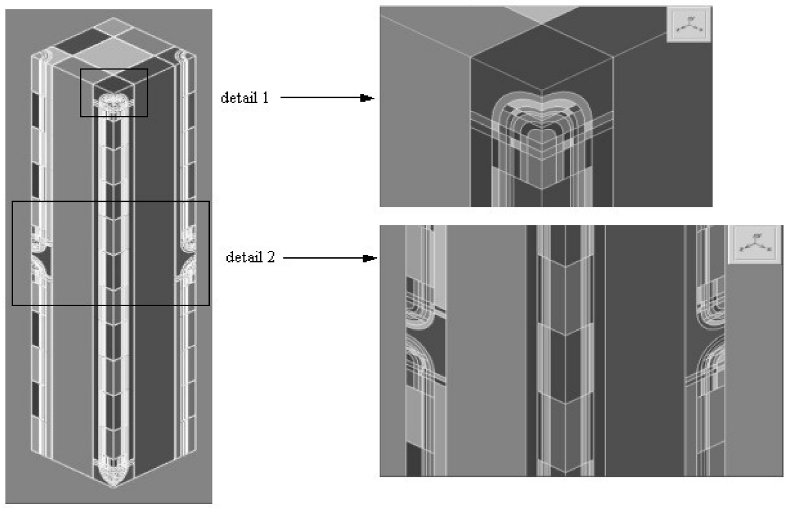

Fig. 3. MEFEA model (3 vol.% of fibres) for matrix and fibre modulus of elasticity ratio $1 : 10^2$, $1 : 10^3$, $1 : 10^4$ – 534 subdomains.

modelled region (control volume – CV) can be used for evaluation of the reinforcing effect.

Figure 2 gives dimensions of the model, Fig. 3 shows the MEFEA model with details of "mesh" and Fig. 4 shows arbitrary shapes of used Apanovitch elements (subdomains). For the numerical simulations of the composite with FEM the model

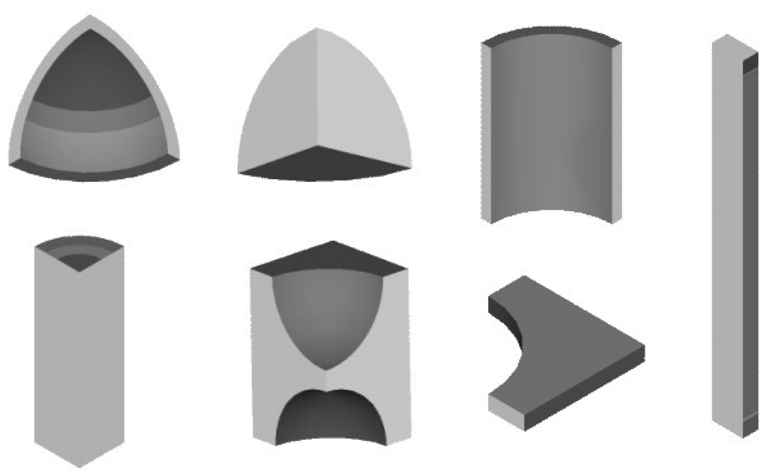

Fig. 4. Arbitrary Apanovitch elements shapes.

contains 4 628 tetrahedrons for matrix and fibre modulus of elasticity ratio $1:10^2$, $1:10^3$, $1:10^4$ in comparison with 534 Apanovitch elements.

3.2 Reinforcing effect

The total force acting on the composite is the sum of forces carried by each constituent (composite – c, matrix – m, fibre – f):

$$F^{\mathrm{c}} = F^{\mathrm{m}} + F^{\mathrm{f}}. \tag{14}$$

The reinforcement in fibre direction r_y, i.e. in the direction of the largest reinforcing effect, can be calculated as follows:

$$r_y = \frac{F_y^{\mathrm{c}}}{F_y^{\mathrm{m}}} = \frac{E_y^{\mathrm{c}}}{E_y^{\mathrm{m}}}, \tag{15}$$

where F_y^{c} is the resultant force which is obtained from the MEFEA and p-FEM model (homogenized total force acting in the cross-section area perpendicular to the fibre direction y) and F_y^{m} is the total force acting on matrix in the cross-section area perpendicular to the fibre direction y, E_y^{c} is homogenized modulus of elasticity of the composite in the fibre direction and E_y^{m} is modulus of elasticity in fibre direction of matrix.

The homogenized average (h-aver) stress $\sigma_{yy}^{\text{h-aver}}$ in fibre direction can be estimated from the homogenized total force F_y^{c} acting in the cross-section area perpendicular to the fibre direction y and the cross-sectional area A_{xz} as:

$$\sigma_{yy}^{\text{h-aver}} = \frac{F_y^{\mathrm{c}}}{A_{xz}} = E_y^{\mathrm{c}} \varepsilon_{yy}^{\mathrm{c}} \qquad \Rightarrow \qquad E_y^{\mathrm{c}} = \frac{\sigma_{yy}^{\text{h-aver}}}{\varepsilon_{yy}^{\mathrm{c}}}, \tag{16}$$

where $\varepsilon_{yy}^{\mathrm{c}}$ is homogenized strain component (the other homogenized strain components are zero for this case: $\varepsilon_{xx} = \varepsilon_{zz} = \varepsilon_{yz} = \varepsilon_{xz} = \varepsilon_{xy} = 0$). The homogenized strain $\varepsilon_{yy}^{\mathrm{c}}$ can be obtained from the displacement of the upper part of the CV.

The computed reinforcement in fibre direction r_y is 1.95 for the model containing 1.2 vol.% of the volume of the composite material and 2.70 for the model containing 3 vol.% for the ratio of matrix to fibre modulus of elasticity equal to $1:10^2$ and for the ratio of radius to length of fibres equal to $1:50$.

3.3 Mechanical behaviour of fibre-reinforced composite

The results obtained by computational models containing 1.2 vol.% of short fibres using MEFEA (Apanovitch elements) and the isoparametric FEM [14] with the p-refinement (pFEM) are presented in the next part.

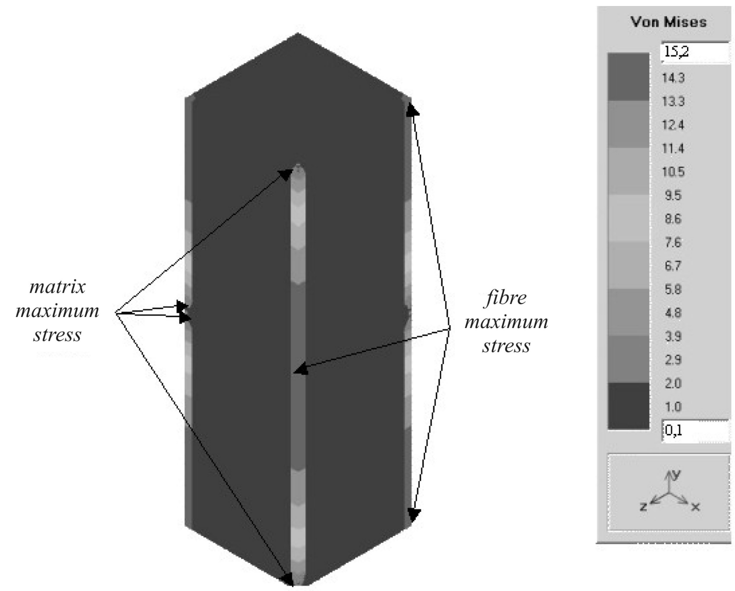

Fig. 5. Stress von Mises-Apanovitch elements.

Figure 5 shows Stress von Mises plot for matrix and fibre modulus of elasticity ratio 1 : 10^2 modelled by Apanovitch elements ($\sigma_{\max}^{\mathrm{MISES}} = 15.2$). The computed value of Stress von Mises achieved by p-elements is $\sigma_{\max}^{\mathrm{MISES}} = 13.6$.

3.3.1 The fields along the fibre boundaries

Figure 6 shows displacement u_y along the fibre boundaries (between points A and B in Fig. 2) for matrix and fibre modulus of elasticity ratio $1 : 10^2$ modelled

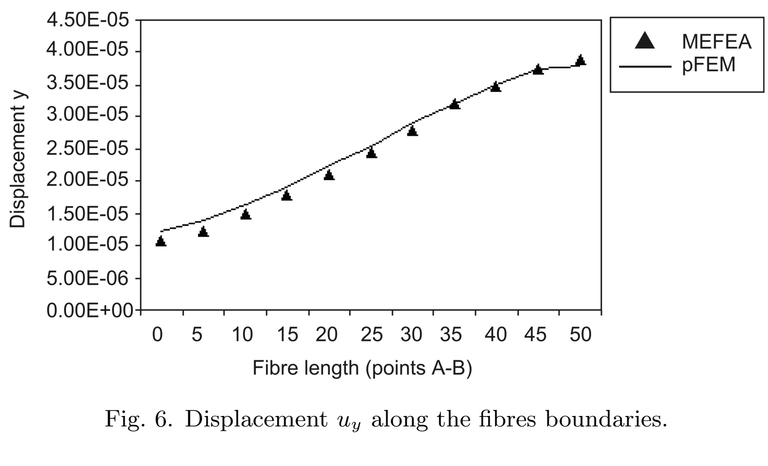

Fig. 6. Displacement u_y along the fibres boundaries.

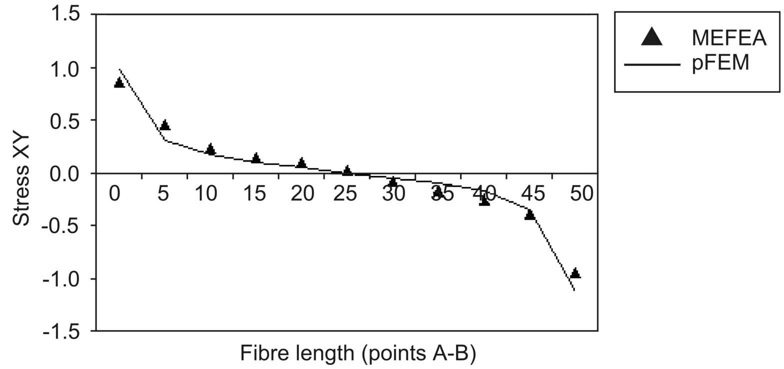

Fig. 7. Stress τ_{xy} along the fibres boundaries.

by Apanovitch elements ($u_{y\ \max} = 3.894 \cdot 10^{-5}$) and p-elements ($u_{y\ \max} = 3.893 \cdot 10^{-5}$), (the point A is in the left side). The difference is 0.026 %.

Figure 7 shows stress XY τ_{xy} along the fibre boundaries for matrix and fibre modulus of elasticity ratio 1 : 10^2 modelled by Apanovitch elements ($\tau_{xy\ \max} = 0.86$) and p-elements ($\tau_{xy\ \max} = 0.99$), (the point A is in the left side). The difference is 13.13 %.

3.3.2 The results along the fibre axis

Figure 8 shows the Stress von Mises along the fibre axis (between points C and D in Fig. 2) for matrix and fibre modulus of elasticity ratio 1 : 10^2 modelled by Apanovitch elements ($\sigma_{\max}^{\text{MISES (fibre axis)}} = 14.74$) and p-elements ($\sigma_{\max}^{\text{MISES (fibre axis)}} = 13.40$), (the point C is in the left side). The difference is 10 %.

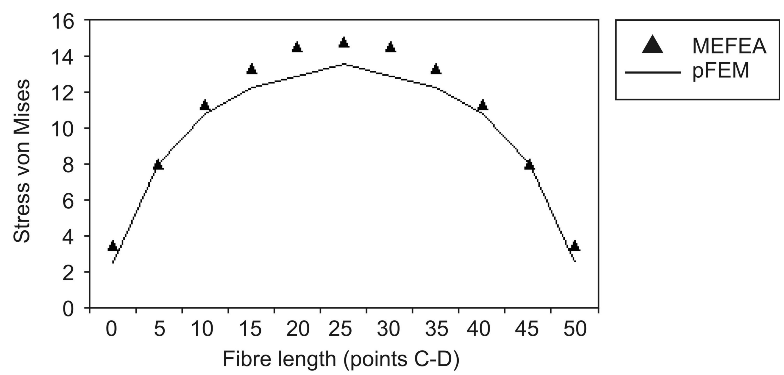

Fig. 8. Stress von Mises along the fibre axis.

3.3.3 Effect of matrix/fibre stiffness ratio

Resulting from analyses, the displacements and stresses are very sensitive to the change of matrix/fibre stiffness ratio. The interface shear stress, responsible for de-cohesion, is one of parameters that are sensitive to the change of matrix/fibre stiffness ratio and also influence local and global behaviour of composite. The stress in fibre is more sensitive to the change of matrix/fibre stiffness ratio compared to stresses in the matrix (Table 2).

Table 2. Effect of matrix and fibre modulus on elasticity ratio

	$E^{m} : E^{f}$	Max. displacement u_y	Max. stress τ_{xy}	Max. Stress von Mises
p-elements	1:10^2	$\mathbf{3.893 \times 10^{-5}}$	0.99	13.4
	1:10^3	2.831×10^{-5}	1.90	29.4
	1:10^4	2.581×10^{-5}	**2.10**	**33.1**

4. Conclusions

In this paper, the computational simulation of composite material reinforced with short fibres was performed using classical displacement FEM formulation using p-refinement and a Trefftz-type FEM formulation called the Method of External Finite Element Approximation (MEFEA). The reinforcing fibres are considered to be unidirectional, straight and regularly distributed so that symmetry conditions can be used to reduce the models. Some overlap is assumed between the fibres. The stiffness of fibres is higher than the stiffness of matrix by two to four orders in our examples.

The shear stresses on the surface between fibres and matrix are responsible for the de-cohesion and the forces in fibres are critical for their load carrying capacity in the composite. The stresses in fibres with large aspect ratio can exceed the stresses in the matrix by several orders. This is an important property of fibre- or tube-type reinforcements. The optimal aspect ratio would be such by which both matrix and material would achieve their strength values by decisive load conditions of the material. p-FEM gave both lower forces in fibres and shear, stresses on the surface between the fibre and the matrix than corresponding values obtained by the MEFEA. This can indicate better accuracy of the last method. Also the computational time is smaller when Trefftz-type elements are used.

In this paper we wanted to show that the Trefftz-type elements using special functions, which better approximate special type of domain such as composite materials with inclusions, enable to reduce the problem. The other aim was to show the influence of fibres on the displacement and stress fields in the matrix. We want to continue in this research and the present results will be used for further development of simulation materials with microstructure.

REFERENCES

[1] APANOVITCH, V. N.: The Method of External Finite Element Approximation. Minsk, Vyshehjshaya Shkola 1991 (in Russian).

[2] AUBIN, J. P.: Approximation of Elliptic Boundary Value Problems. New York, Wiley – Interscience 1972.

[3] BELYTSCHKO, T.—LIU, W. K.—MORAN, B.: Nonlinear Finite Elements for Continua and Structures. Chichester, John Wiley & Sons, Ltd. 2000.

[4] CÉA, J.: Ann. Inst. Fourier, *14*, 1964, p. 345.

[5] GAUL, L.—MOSER, F.: A Hybrid Boundary Element Approach without Singular Boundary Integrals, Selected Topics in Boundary Integral Formulations for Solids and Fluids. Ed.: Kompiš, V. Wien, Springer 2002, p. 107.

[6] GOLBERG, M. A.—CHEN, C. S.: The Method of Fundamental Solutions for Potential, Helmholtz and Diffusion Problems. Boundary Integral Methods – Numerical and Mathematical Aspect. Ed.: Golberg, M. A. Southampton, Computational Mechanics Publications 1998, p. 103.

[7] JIROUSEK, J.—WROBLEWSKI, A.: Archive of Applied Mechanics, *3*, 1997, p. 323.

[8] KARAGEORGHIS, A.—FAIRWEATHER, G.: IMA Journal Numerical Analysis, *9*, 1989, p. 231.

[9] KOMPIŠ, V.—ŠTIAVNICKÝ, M.: Computer Assisted Mechanics and Engineering Sciences, *13*, 2006, p. 417.

[10] MA, H.—QIN, Q. H.: Boundary Point Method for Linear Elasticity Based on Direct Formulations of Conventional and Hypersingular Boundary Integral Equations (to be published).

[11] NISHIMURA, N.—LIU, Y. L.: Computation Mechanics, *35*, 2004, p. 1.

[12] QIN, Q. H.: The Trefftz Finite and Boundary Element Method. Southampton, WIT Press 2000.

[13] SHONAIKE, G. O.—SURESH, A.: Advanced Polymeric Materials: Structure Property Relationship. Boca Raton, CRC Press 2003.

[14] ZIENKIEWICZ, O. C.—TAYLOR, R. L.: The Finite Element Method. 5th ed. Oxford, Butterworth-Heinemann 2000.

Received: 28.9.2007
Revised: 8.1.2008